Comparison of *s*- and *d*-wave gap symmetry in nonequilibrium superconductivity

E. J. Nicol
Department of Physics, University of Guelph, Guelph, Ontario, Canada N1G 2W1

J. P. Carbotte
Department of Physics and Astronomy, McMaster University, Hamilton, Ontario, Canada L8S 4M1

(Received 19 August 2002; revised manuscript received 26 December 2002; published 9 June 2003)

Recent application of ultrafast pump/probe optical techniques to superconductors has renewed interest in nonequilibrium superconductivity and the predictions that would be available for novel superconductors, such as the high-T_c cuprates. We have reexamined two of the classical models which have been used in the past to interpret nonequilibrium experiments with some success: the μ^* model of Owen and Scalapino and the T^* model of Parker. Predictions depend on pairing symmetry. For instance, the gap suppression due to the excess quasiparticle density n in the μ^* model, varies as $n^{3/2}$ in d wave as opposed to n for s wave. Finally, we consider these models in the context of S-I-N tunneling and optical excitation experiments. While we confirm that recent pump/probe experiments in YBCO, as presently interpreted, are in conflict with d-wave pairing, we refute the further claim that they agree with s wave.

DOI: 10.1103/PhysRevB.67.214506 PACS number(s): 74.72.−h, 74.40.+k, 74.25.Gz

I. INTRODUCTION

The field of nonequilibrium superconductivity was very active throughout the late 1970's to mid-1980's when it was realized that novel effects in the superconducting state could be induced by converting the electron distribution function into a nonequilibrium one.[1] Different experimental techniques were used to prepare such a nonequilibrium state, for example, tunnel injection and optical irradiation, and a body of work arose from both experimental and theoretical efforts in this area. A useful summary of this work near the end of this period of time can be found in a book edited by Langenberg and Larkin[1] and other broad-based texts have also appeared more recently.[2,3]

The advent of high-T_c cuprate superconductivity in 1986 interrupted work in this and other areas as the community turned its attention to this new challenge and, consequently, extensive work in the area of nonequilibrium superconductivity has languished until more recently. However, during the period following the original burst of activity, new state-of-the-art experimental probes have been developed which provide excellent opportunities for renewed interest in this field, not to mention the potential for new insights provided by the new generation of materials exhibiting novel superconductivity, such as the cuprates. Some of these probes which can be turned to this problem are STM, ultrafast lasers, spin-polarized tunneling injection, terahertz spectroscopy, etc.

As early as the mid-1980's, the pump/probe femtosecond spectroscopy was exhibiting its potential as a technique for investigating nonequilibrium phenomena in metals and superconductors. In these experiments, an ultrafast laser pulse (~100 fs) incident on a sample as a high energy ''pump'' quickly excites the electrons out of equilibrium which then relax back to thermal equilibrium with the lattice via the electron-phonon interaction. Another laser pulse delayed in time ''probes'' the system of electrons by reflection or transmission spectroscopy. As the system of electrons relaxes, the transient reflectivity or transmissivity decays with time over a scale of picoseconds or less allowing this experiment to probe carrier dynamics in a time-resolved fashion. A theory was proposed by Allen[4] for the relaxation of quasiparticles in the normal state, which could be measured in these experiments, resulting in the extraction of the electron-phonon renormalization parameter λ (as the quasiparticles relax through interactions with the system of phonons). Experiments were performed which measured this parameter using Allen's theory and excellent agreement was found with other values in the literature for both ordinary metals and superconductors in the normal state.[5] Indeed, this parameter was measured for the first time in Cr by this technique.[5] This extraordinary success has led experimentalists to use the femtosecond laser as a probe of high temperature superconductivity[6–10] and in general several groups have been developing ultrafast techniques of similar sort for measuring nonequilibrium phenomena in superconductors.[11,12]

Here, we are interested in the state that arises when the nonequilibrium excitations, created by a laser pulse or by tunneling injection, have fallen to the gap edge but have not yet recombined into the condensate (bottleneck effect). In the first case, there is some debate amongst experimentalists as to whether the high energy laser used for pumping and probing can truly measure the distribution of quasiparticles at low energy and several groups are developing techniques to probe at lower energy of order of the gap to address this issue.

The main thrust of our work has involved the use of two models employed in the past to describe a nonequilibrium distribution of quasiparticles: the T^* model of Parker[13] which uses an equilibrium distribution function at an effective temperature T^* relative to the bath temperature T and the μ^* model, originally proposed by Owen and Scalapino,[14] where the system is described in terms of a new chemical potential for the excited quasiparticles. The former approach

has been used by Kabanov *et al.*[7] to analyze their optical data, whereas the latter approach has been used for systems where excess particles are injected into tunnel junctions.[15] While these two models are somewhat simplified, they appear to have been effective in capturing some of the experimental results on low T_c superconductors.

In Sec. II, we calculate how the superconductivity is modified as a function of the nonequilibrium excess quasiparticle number density n. This leads to modifications in the gap which we calculate numerically for various values of temperature T characterizing the sample before irradiation as a function of n in both μ^* and T^* models and for s- and d-wave. For $T=0$ and in the limit of $n\to 0$, we also obtain analytic results for the gap reduction versus n, for the chemical potential in the μ^* model and for the nonequilibrium effective temperature for the T^* model, as well as for the free energy difference between the nonequilibrium superconducting state and the corresponding equilibrium normal state. The analytic limits are tested against the numerical work and found to be close to the exact results even as n increases towards its critical value where superconductivity is destroyed. Results for d wave are compared with s waves and important differences are established. In Sec. III, as an explicit example of an application of our results, we consider a S-I-N tunneling junction with a nonequilibrium state on the superconducting side which we assume can be described by a μ^* model. We show that the current voltage characteristics are modified in two major ways. First the amplitude of the gap is reduced because of the presence of a nonequilibrium number of excess quasiparticles n and secondly the entire characteristic is shifted upward by a factor of n in appropriate units. Also the voltage at which the current is zero can be used to measure the chemical potential μ^*. Separate measurements of the gap reduction, the chemical potential, and the upward shift in I-V characteristic would allow a consistency test of the model. In Sec. IV, we consider the specific case of pump/probe experiments and agree with previous theoretical work[7] that the existing data, as currently interpreted, is not consistent with d-wave gap symmetry, but disagree that it is consistent with s wave. In Sec. V, we draw conclusions and give a summary of our results.

II. THEORY

We consider two models used in the past for the treatment of nonequilibrium superconductivity. For an s-wave BCS superconductor, Owen and Scalapino considered a state in which there exists a finite distribution of excess quasiparticles at the gap energy in addition to a condensate. In their μ^* model,[14] thermal equilibrium is assumed although chemical equilibrium is not for the paired and unpaired electrons. This is mimicked through the introduction of a chemical potential μ^* in the Fermi function which represents a constraint on the quasiparticle excitation number. With this chemical potential the Fermi function is

$$f(E_k-\mu^*)=[1+\exp\beta(E_k-\mu^*)]^{-1} \tag{1}$$

with the BCS gap equation modified to be

$$\frac{1}{N(0)V}=\int_0^{\omega_c}\frac{d\epsilon_k}{\sqrt{\epsilon_k^2+\Delta^2(n)}}\tanh[\beta(E_k-\mu^*)/2], \tag{2}$$

where V is the pairing potential, $N(0)$ is the electronic density of states at the Fermi surface in the normal state, and the excess quasiparticle density n is given as

$$n=\frac{1}{\Delta(0)}\int_0^{\infty}[f(E_k-\mu^*)-f(E_k)]d\epsilon_k, \tag{3}$$

where $\beta=1/(k_BT)$, $E_k=\sqrt{\epsilon_k^2+\Delta^2(n)}$, and k_B is the Boltzmann constant. Here n is measured in units of $4N(0)\Delta(0)$. The 4 is introduced for spin and for particle-hole parts of the excitation spectrum. $\Delta(0)\equiv\Delta(n=0)$ is the superconducting gap in the equilibrium state, finite and isotropic over the entire Fermi surface for s-wave gap symmetry.This model will be applied later to discuss tunneling.

Alternatively, Parker[13] considered a T^* model where instead of a μ^* in the Fermi function, a T^* is used:

$$f(E_k,T^*)=[1+\exp(E_k/k_BT^*)]^{-1} \tag{4}$$

with the other equations modified accordingly. This model is the one used by Kabanov *et al.*[7] in their analysis of the pump/probe data.

We consider first, the μ^* model for an s-wave BCS superconductor. At zero temperature the existence of the excess quasiparticles perturb the condensate by blocking states which would otherwise be available to form the condensate in a variational sense, and this lowers the value of the gap. The exact gap equation and relationship between chemical potential and n are, respectively,

$$\frac{\Delta(n)}{\Delta(0)}=\left(\frac{\mu^*}{\Delta(0)}+n\right)^2 \quad\text{and}\quad n\Delta(0)=\sqrt{\mu^{*2}-\Delta^2(n)}. \tag{5}$$

The first expression in Eq. (5) comes directly from the gap equation (2) evaluated at zero temperature with reference made to the equilibrium case which allows us to eliminate the pairing potential in favor of $\Delta(0)$. The second follows from Eq. (3). The grand potential $\Omega^S(n)$ [the familiar formula is given later for the anisotropic case in Eq. (13)] in the isotropic case (at $T=0$) is

$$\frac{\Delta\Omega(n)}{N(0)}\equiv\frac{\Omega^S(n)-\Omega^N(0)}{N(0)}$$
$$=-\frac{1}{2}\Delta^2(n)-2\mu^*\sqrt{\mu^{*2}-\Delta^2(n)}, \tag{6}$$

where this is the difference between the nonequilibrium superconducting state and its normal equilibrium counterpart (i.e., with no excess quasiparticles). The difference normalized to the equilibrium superconducting state condensation energy is

$$\frac{2\Delta\Omega(n)}{N(0)\Delta^2(0)}=\frac{2[\Omega^S(n)-\Omega^N(n=0)]}{N(0)\Delta^2(0)}\approx -1+8n^2 \tag{7}$$

TABLE I. Analytical forms for $n\to 0$ at $T=0$ in the μ^* model. Note n is in units of $4N(0)\Delta(0)$, where $N(0)$ is the single spin density states and $\Delta(0)$ is the $T=0$ and $n=0$ gap (maximum in d wave).

μ^* model	s wave	d wave
$\Delta(n)/\Delta(0)$	$1-2n$	$1-\frac{4\sqrt{2}}{3}n^{3/2}$
$2\Delta F(n)/N(0)\Delta^2(0)$	$-1+8n$	$-\frac{1}{2}+\frac{16\sqrt{2}}{3}n^{3/2}$
$\mu^*/\Delta(0)$	$1-2n$	$\sqrt{2}n^{1/2}$

to lowest order in n. To obtain Eq. (7) we have used expressions for $\Delta(n)/\Delta(0)$ and for $\mu^*/\Delta(0)$ valid to second order in n. They are $\Delta(n)/\Delta(0)=1-2n-2n^2$ and $\mu^*/\Delta(0)=1-2n-3n^2/2$ (entered in Table I to lowest order). If we add to the grand potential, $\Delta\Omega(n)$, the number of excess quasiparticles multiplied by the chemical potential, i.e., $\mu^*\overline{n}$, where $\overline{n}$ is the first term of Eq. (3), normalized in the same way as Eq. (7), we get the normalized free energy difference at zero temperature which we denote by $2\Delta F(n)/N(0)\Delta^2(0)$. This is evaluated to be

$$\frac{2\Delta F(n)}{N(0)\Delta^2(0)}\simeq -1+8n \tag{8}$$

(entered in Table I).

In the top frame of Fig. 1, we present our numerical results for the ratio $\Delta(n)/\Delta(0)$ as a function of excess quasiparticles n (solid curve) and compare with the approximate result $\Delta(n)/\Delta(0)=1-2n$ (dashed curve). We see excellent agreement at small n. As n is increased, the continuation of the solid curve is denoted by the dots. It is terminated at the point where the free energy for the nonequilibrium state becomes equal to its normal state value and a first order transition occurs. This can be seen more clearly in the bottom frame which shows the normalized free energy difference of the nonequilibrium ($n\neq 0$) state, $2\Delta F(n)/N(0)\Delta^2(0)$ as a function of n. The solid curve applies to the exact result at $T=0$ while the dashed is the approximate result [Eq. (7)] which fits the exact result at small n well and is semiquantitative in the entire physical region. The first order phase transition to the normal state occurs at $n_c\sim 0.15$. The continuation of the solid line for the free energy difference to values of excess quasiparticles n beyond the critical value is indicated by a dotted curve just as in the top frame for the gap. We note that both the gap $\Delta(n)$ and the free energy difference $\Delta F(n)$ as a function of n fold back on themselves beyond a certain value of n, but that the free energy remains positive for the entire dotted region, i.e., the nonequilibrium state has higher free energy than does the normal state $[\Delta F(n)>0]$ in this region.

Now we treat the d-wave case. The equation relating μ^* to n is $n\Delta(0)=\int_0^{\mu^*}\overline{N}(E)dE$ where for small E, $\overline{N}(E)\simeq E/\Delta(n)$. Here, $\Delta(n)$ is the maximum d-wave gap where

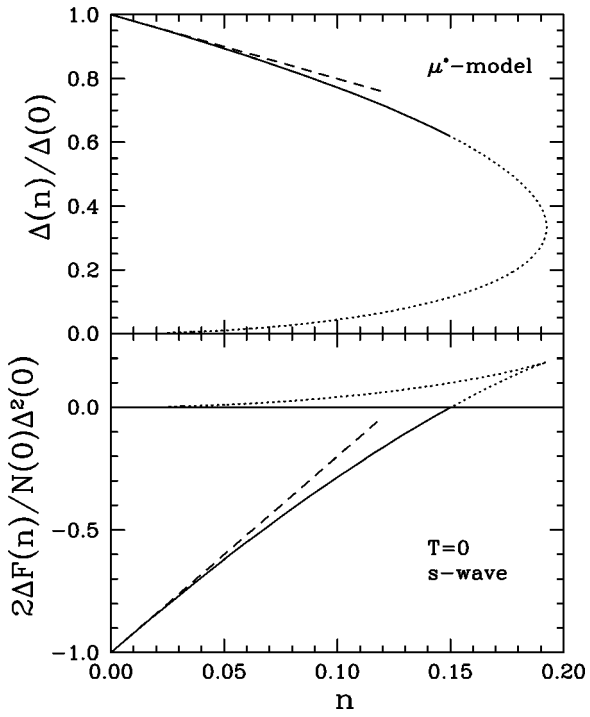

FIG. 1. Top frame: $\Delta(n)/\Delta(0)$ versus n, at $T=0$ for the μ^* model with an s-wave gap. The solid curve is physical, the dotted curve is not. This latter curve represents the case where the free energy of the normal state is lower than that of the superconducting state as shown in the bottom frame. The presence of excess quasiparticles suppresses the gap and eventually leads to a first order transition to the normal state at $n=0.15$. Bottom frame: $\Delta F=F_N-F_S$, the free energy difference, versus n. In both frames, the dashed curve is the small n limit (see Table I).

the gap $\Delta(\phi)$ at any point ϕ (the polar angle for momentum) on the two-dimensional Fermi circle in the CuO_2 Brillouin zone is $\Delta(\phi)=\Delta(n)\cos(2\phi)$ with zeros in the (π,π) direction and other symmetry related points. The small n limit gives $\mu^*/\Delta(0)=\sqrt{2}n^{1/2}$ which differs radically from the s-wave case and reflects the gap symmetry with nodes (see Table I). Numerical results for $\mu^*/\Delta(0)$ versus n are given in Fig. 2. The top frame applies to the s-wave case and is for comparison with the bottom frame for d wave. The dashed curves in both frames are our approximate analytical results which are seen to match well the exact results (solid curve for $T=0$) in the small n limit. The remaining curves are at finite temperature T as indicated in the caption, namely, $T/T_c=0.3$, 0.5, 0.7, and 0.9. Several features are worth noting. For s wave, the zero temperature behavior of the chemical potential as a function of n is qualitatively different from the case for finite temperature. In the limit of $n\to 0$, i.e., very few excess quasiparticles, the chemical potential must clearly be equal to $\Delta(n=0)$ at $T=0$. In this case the lowest energy available quasiparticle states are at $\Delta(0)$ where there is an inverse square root singularity in the density of states and hence all the excess quasiparticles can be accommodated at the gap energy. As n increases out of zero, the gap $\Delta(n)$ in the nonequilibrium state decreases from its value at $n=0$. The inverse square root singularity shifts to lower energy and there are now many states at and around $\Delta(n)$ and it turns

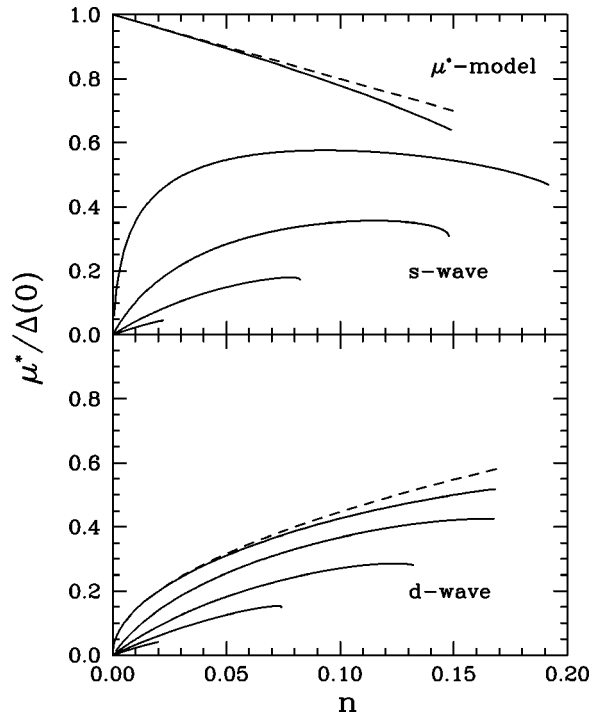

FIG. 2. The parameter μ^* versus n for several temperatures shown for the s-wave (top frame) and d-wave (bottom frame) gaps. The dashed curve is the small n limit (see Table I). From top to bottom, the solid curves are for $T/T_c=t=0$, 0.3, 0.5, 0.7, 0.9. Here only the physical part of the curves are shown.

out that all the excess quasiparticles can be accommodated in a small energy range around the new gap value. We have already noted that to second order in n, $\Delta(n)/\Delta(0)$ and $\mu^*/\Delta(0)$ differ by a factor of $n^2/2$, specifically, $\mu^*/\Delta(0)=[\Delta(n)/\Delta(0)]+n^2/2$ which implies that μ^* falls a few percent above the nonequilibrium value of the gap in units of $\Delta(0)$. Note that the inequality $\Delta(n)/\Delta(0)<\mu^*/\Delta(0)$ (at $T=0$ only), found to hold to second order in n, was also verified in the numerical work, which shows that the difference between $\Delta(n)$ and μ^* are always small even outside the validity of our expansion. That this difference should be small is a reflection of the square root singularity in the density of states.

The situation is very different in the d-wave case and in s wave at finite temperature. In these two cases the chemical potential becomes small as $n\to 0$. For the d-wave case this is easily understood because there is a small but finite density of states at any nonzero value of energy $\omega\neq 0$. The excess quasiparticles can occupy these states and hence $\mu^*\to 0$ as $n\to 0$. For the s-wave case at finite T a different argument holds. In this case the thermal factor $f(E_{\vec{k}}-\mu^*)$ gives the probability that the state $E_{\vec{k}}$ is occupied at finite T. This probability can be increased over its value for $\mu^*=0$ simply by having μ^* take on a small finite value to accommodate the excess quasiparticles. At low temperature, however, the thermal tails of the occupation factor are small in the region of the gap and μ^* must increase fairly rapidly as n increases. This is seen most clearly in the second highest curve in the top frame of Fig. 2 which corresponds to $T/T_c=t=0.3$. Also as the temperature is increased μ^* decreases as expected. In the d-wave case shown in the lower frame of Fig. 2, μ^* starts from zero at $n=0$ even at zero temperature because, as we have already indicated, there are states available at any energy above $\omega=0$. Comparing top and bottom frame we note that the chemical potential for $t=0.3$ (to be specific) rises more rapidly in the s-wave case and becomes bigger than for d wave. This can be traced to the fact that for d wave the part of the density of states that is occupied by the excess quasiparticles is in the range 0 to μ^* while in the s wave case it is the region just about the gap $\Delta(n)$ which is relevant. As the temperature is increased towards T_c, the differences in the quasiparticle density of states between s and d wave become smaller and the chemical potentials start to become very similar. A second feature to be noticed is that at finite T the curves for μ^* extend to higher values of n for the s-wave case than they do in the d-wave case although the reverse is true at zero temperature. In all cases the curves terminate when the free energy difference between normal and nonequilibrium superconducting state becomes zero or there are two solutions and the one with the lowest free energy is chosen. This occurs at smaller values of n for the d-wave case as compared with s wave for the given temperature $T\neq 0$ shown. We will return to this issue later on in our discussion of Fig. 4.

The gap equation with a pairing potential of the form $V_{\mathbf{k}\mathbf{k}'}=V\cos(2\phi')\cos(2\phi)$, where $\mathbf{k}$ is momentum on the Fermi surface, with a distribution of excess quasiparticles included through the introduction of a chemical potential takes the form

$$\frac{1}{N(0)V}=\left\langle 2\int_0^{\omega_c}\frac{\cos^2(2\phi)d\epsilon_k}{\sqrt{\epsilon_k^2+\Delta^2(n)\cos^2(2\phi)}}\times\tanh[\beta(E_k-\mu^*)/2]\right\rangle \tag{9}$$

with $E_k=\sqrt{\epsilon_k^2+\Delta^2(n)\cos^2(2\phi)}$. The bracket $\langle\cdots\rangle$ indicates the angular average and ϵ_k is energy integrated in a rim of width ω_c about the Fermi energy. With reference to the $n=0$ case (i.e., $\mu^*=0$) we can rewrite Eq. (2) to read at $T=0$

$$\ln\left(\frac{\Delta(n)}{\Delta(0)}\right)=-4\left\langle\int_0^{\omega_c}\frac{\cos^2(2\phi)d\epsilon}{\sqrt{\epsilon^2+\Delta^2(n)\cos^2(2\phi)}}\right\rangle_{E_k\leqslant\mu^*}, \tag{10}$$

where the integration over energy and ϕ must duly take account of the restriction $E\leqslant\mu^*$. For small $n\to 0$ the leading order gives $[\Delta(n)=\Delta(0)+\delta\Delta(n)]$

$$\frac{\delta\Delta(n)}{\Delta(0)}=-\frac{8}{\pi}\int_{\cos^{-1}(\mu^*/\Delta(n))}^{\pi/2}\cos^2\phi'd\phi'\times\int_{|\Delta(n)\cos\phi'|}^{\mu^*}\frac{dE}{\sqrt{E^2-\Delta^2(n)\cos^2\phi'}}, \tag{11}$$

where we have changed from ϕ to $\phi'=2\phi$. But the lower limit in the ϕ' integration in Eq. (11) restricts the integration to the nodal region which corresponds to $\phi'=\pi/2$. We find

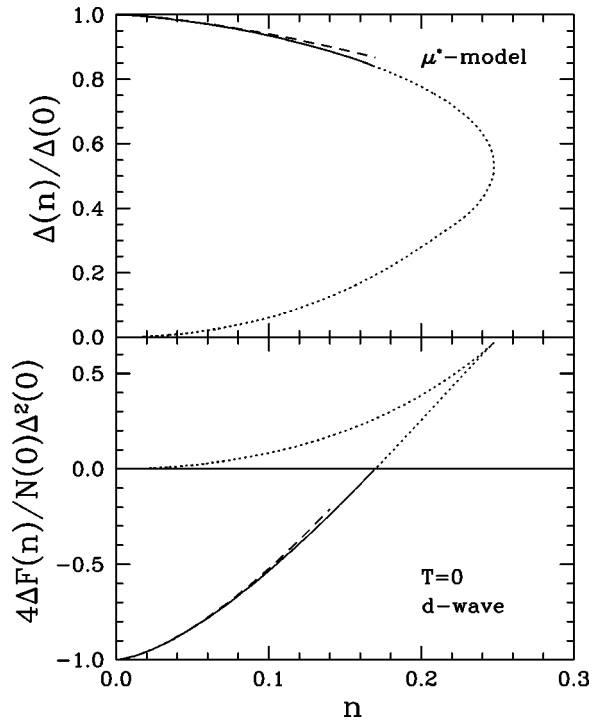

FIG. 3. The μ^* model at $T=0$ for a *d*-wave gap with the curves labelled in the same manner as for Fig. 1. The gap is suppressed less rapidly in *d* wave. The presence of excess quasiparticles, which normally weaken the condensate by blocking states, are less effective in interfering with the formation of the superconducting wavefunction in *d*-wave as they accumulate at the nodes, in the first instance, which is a region where the gap is close to zero.

$$\frac{\delta\Delta(n)}{\Delta(0)} = -\frac{8}{\pi}\left(\frac{\mu^*}{\Delta(n)}\right)^3 \int_0^1 x^2 dx \ln\left|\frac{1+\sqrt{1-x^2}}{x}\right| \simeq -\frac{4\sqrt{2}}{3} n^{3/2} \tag{12}$$

(entered in Table I) where we have used the relationship $\mu^*/\Delta(n)=\sqrt{2}n^{1/2}$ to lowest order. In Fig. 3 we show exact numerical results for the normalized gap $\Delta(n)/\Delta(0)$ as a function of n for the *d*-wave case (solid curve) and compare with our approximate result (dashed curve) which applies only at small n. The agreement is excellent even up to the point where the first order transition to the normal state occurs. This is where the solid curve is extended into the dotted curve. The gap function as a function of n is reduced less in *d* wave (Fig. 3) as compared to *s* wave (Fig. 1) all the way to $n=n_c$. The free energy difference $\Delta F(n)$ becomes zero at $n=n_c\simeq 0.17$ which is to be compared with $\simeq 0.15$ in the *s*-wave case. At the critical n, $\Delta(n)/\Delta(0)$ is almost 0.6 for *s* wave while in the *d*-wave case it has not yet reached 0.8. The blocking of states by the excess quasiparticles has much less effect on the condensate wave function as reflected in the change in the value of the gap in *d* wave than in *s* wave because now the excess quasiparticles accumulate in the nodal region. Since the gap is zero or near zero in that region, it is clear that these states do not contribute much to the lowering of energy brought about by the formation of Cooper pairs.

To establish where this first order transition occurs, we need the free energy. The formula for the grand potential for the superconducting state with n excess quasiparticles is

$$\Omega^S(n) = 2k_BT\sum_k \ln[1-f(E_k-\mu^*)] + \sum_k \left[\epsilon_k - E_k + \frac{\Delta_k^2}{2E_k}[1-2f(E_k-\mu^*)]\right] \tag{13}$$

and for the normal state with $n=0$ it is

$$\Omega^N(0) = 2k_BT\sum_k \ln[1-f(|\epsilon_k|)] + \sum_k (\epsilon_k - |\epsilon_k|). \tag{14}$$

The sum over $\mathbf{k}$ can be converted to energy and the constant two dimensional electron density of states factor $N(0)$ taken out of the integration. In the limit $n\to 0$

$$\frac{\Delta\Omega(n)}{N(0)} \equiv \frac{\Omega^S(n)-\Omega^N(0)}{N(0)} = -\frac{1}{4}\Delta^2(n) + 4\int_0^{\mu^*} \overline{N}(E)(E-\mu^*)dE - \frac{1}{2}I\Delta^2(n), \tag{15}$$

where I is the same integral as appears on the right-hand side of Eq. (11). The first term in Eq. (15) is the usual expression for the condensation energy of a *d*-wave superconductor but with $\Delta(n)=\Delta(0)(1-4\sqrt{2}n^{3/2}/3)$ replacing the gap amplitude $\Delta(0)$ which applies to $n=0$. In $\Delta\Omega(n=0)/N(0)$ only $\Delta^2(0)/4$ enters. The two extra terms in Eq. (15) can be worked out analytically as $n\to 0$ and lead to

$$\frac{\Delta\Omega(n)}{N(0)} = -\frac{1}{4}\Delta^2(n) - \frac{2}{3}\frac{\mu^{*3}}{\Delta(n)} - \frac{1}{3}\left(\frac{\mu^*}{\Delta(n)}\right)^3\Delta^2(n), \tag{16}$$

only in the first term on the right-hand side of the equation must we retain the n dependence in $\Delta(n)$. The difference in grand potential $\Delta\Omega(n)$ normalized to $\Delta^2(0)N(0)/4$ is easily worked out to be

$$\frac{4\Delta\Omega(n)}{N(0)\Delta^2(0)} = -1 - \frac{16\sqrt{2}}{3}n^{3/2}. \tag{17}$$

The normalized free energy ΔF is obtained by adding $\mu^*\overline{n}$ to Eq. (13) and after normalization we get

$$\frac{4\Delta F(n)}{N(0)\Delta^2(0)} = -1 + \frac{32\sqrt{2}}{3}n^{3/2} \tag{18}$$

which is entered in Table I. Numerical results at any value of n are shown in the bottom frame of Fig. 3. The solid line is our numerical result for $4\Delta F(n)/N(0)\Delta^2(0)$ at $T=0$ and the dashed curve our approximate result [Eq. (18)]. The analytic result agrees well with the full numerical solution at

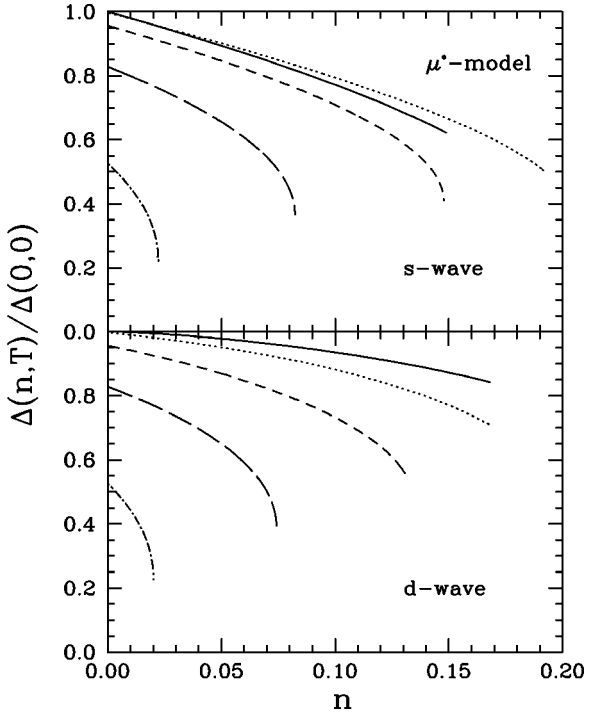

FIG. 4. The ratio of $\Delta(n,T)/\Delta(0,0)$ versus n for finite temperature in the μ^* model. The top frame is for the case of an s-wave gap and the bottom frame is for d wave. Curves are shown for $T/T_c = t = 0$ (solid curve), 0.3 (dotted), 0.5 (short-dashed), 0.7 (long-dashed), 0.9 (dot-dashed). Only the physical part of the curves are shown.

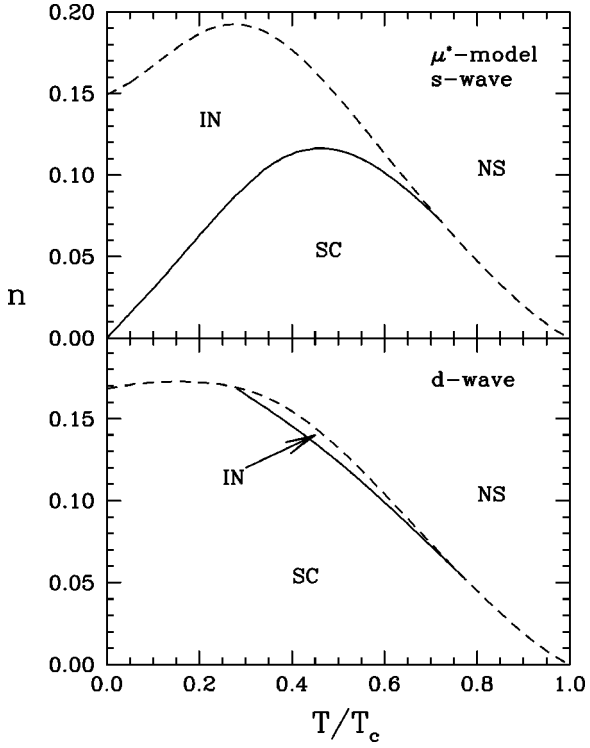

FIG. 5. The phase diagrams calculated in the the μ^* model for the s-wave (top) and d-wave (bottom) gaps. Based on the slope of μ^* versus n one can determine the region of the phase diagram where there is a homogeneous (SC) and an inhomogeneous superconducting state (IN). The transition from the superconducting state to the normal state (NS) is always first order and is represented by the dashed line.

small n and differs slightly near the critical value of $n = n_c$ where the first order transition to the normal state occurs at $n_c \approx 0.17$.

In Fig. 4 we show our numerical results for the gap as a function of n at various temperatures. Both frames are for the μ^* model. The temperatures are $T/T_c = t = 0$ (solid curve), 0.3 (dotted), 0.5 (short dashed), 0.7 (long dashed), and 0.9 (dot dashed). The top frame is for s wave and is for comparison with the bottom frame which is new and applies to d wave. Note that for s wave, the $T = 0$ curve is below the dotted curve for $t = 0.3$. This agrees with findings of Owen and Scalapino and has its origin in the blocking process referred to previously. At zero temperature the excess quasiparticles block important states which cannot be used in the coherent superposition of states which form the Cooper pair condensate. At finite temperature the blocking is less effective because it is the states closest to zero energy that are the most effective in forming the condensed pairs while the thermal factor depopulates these states. By contrast, for d wave, the $T = 0$ curve is above the $t = 0.3$ (dotted curve) as we have already noted. In this instance the blocking at $T = 0$ is much less effective and consequently temperature is not as important an effect. We note again that, at $T = 0$, the d-wave gap is reduced less than in s-wave for the same value of n and that the critical value of n, at which a first order transition to the normal state takes place, is larger. At the higher temperatures shown, however, the reverse holds. Also, note that as the temperature rises towards T_c the difference between s and d wave get less pronounced as the differences between the two quasiparticle density of states become small and also more states are involved.

The nonthermal quasiparticle distribution used in the μ^* model has an interesting aspect in that it allows for the system to become unstable to quasiparticle density fluctuations.[16,17] Essentially, if the quasiparticles are injected uniformly in the sample, the density fluctuations will act to draw off quasiparticles from some regions thereby increasing the superconducting gap locally and flowing those quasiparticles to other regions, causing an accumulation which lowers the local gap, possibly even driving the local region normal. This phase separation could be either a static or a temporal structure. Such a state has been studied initially by Chang and Scalapino[16] and Scalapino and Huberman[17] for the s-wave superconductor and experimental verification of a density instability leading to an inhomogeneous multigap state has been done by several groups[18] using tunnel injection in thin film nonequilibrium superconductors. The theoretical signature of such an inhomogeneous state in the μ^* model is that $\partial\mu^*/\partial n|_T < 0$.[16,17] From Fig. 2, we find that the variation of μ^* with n differs in s and d wave and by examining the slopes of these curves, in particular, the point where the slope goes negative, we can reproduce the s-wave phase diagram of Chang and Scalapino,[16] shown in the upper frame of Fig. 5, and provide the equivalent prediction for d wave in

the bottom frame. The dashed curve in these phase diagrams marks the boundary between the normal state (NS) and the superconducting state (either homogeneous or inhomogeneous). This boundary is entirely a first-order transition. The area labeled IN, is the region of n and T, where the slope of the chemical potential curve is negative and an inhomogeneous state is predicted to exist. The solid line marks the boundary between it and the homogeneous superconducting state (SC). There are qualitative differences between the *s*- and *d*-wave cases. The region of the inhomogeneous phase is quite large in the *s*-wave case and almost nonexistent in *d* wave and at low temperature the *s*-wave superconductor would likely be phase separated whereas, the *d*-wave one would not be. While the inhomogeneous state may be of interest to study in itself, in the *d*-wave case it may be encouraging to note that attempts at experimental verification of our predictions for power law dependences, and other results presented in this paper, are unlikely to be hampered by the presence of an inhomogeneous phase.

Next we consider briefly the case of the T^* model which is just a simple heating model if only the electronic system is considered. Similar approximate analytic calculations can be done to get various relationships in the limit $n \to 0$ for the case when the sample before irradiation is assumed to be zero. These analytic derivations are supplemented with full numerical work in which we also consider the case when the sample is initially at finite temperature T.

We begin with the *s*-wave case and return to the gap equation shown in Eq. (2), now modified according to Eq. (4) rather than Eq. (1). In the limit of $T \to 0$, the result for the lowest order correction to the gap is well known:[19]

$$\frac{\delta\Delta(n)}{\Delta(0)} = -\sqrt{\frac{2\pi k_B T^*}{\Delta(0)}} e^{-\Delta(0)/k_B T^*}. \tag{19}$$

The relation between n and T^* can be trivially obtained as $n = \sqrt{\pi T^*/2\Delta(0)} e^{-\Delta(0)/k_B T^*}$ and so $\delta\Delta(n)/\Delta(0) = -2n$.

The *d*-wave case is not as well known and we include the critical steps here

$$\ln\left(\frac{\Delta(n)}{\Delta(0)}\right) = -4\int_0^{\pi/2} \frac{2\,d\phi'}{\pi} \cos^2\phi' \times \int_{\Delta(n)\cos\phi'}^{\omega_c} \frac{dE}{\sqrt{E^2 - \Delta^2(n)\cos^2\phi'}} e^{-E/k_B T^*} \tag{20}$$

which can be manipulated into

$$\ln\left(\frac{\Delta(n)}{\Delta(0)}\right) = -\frac{8}{\pi}\int_0^{\pi/2} d\phi \cos^2\phi' e^{-\Delta(n)\cos\phi'/k_B T^*} \times \int_0^{\omega_c} \frac{dx\, e^{-x/k_B T^*}}{\sqrt{x[x + 2\Delta(n)\cos\phi']}}. \tag{21}$$

The integral over ϕ' is peaked around $\cos\phi' = 0$, i.e., ϕ' near $\pi/2$ which allows us to approximate it by

TABLE II. Analytical forms for $n \to 0$ at $T = 0$ in the T^* model. Note n is in units of $4N(0)\Delta(0)$, where $N(0)$ is the single spin density states and $\Delta(0)$ is the $T = 0$ and $n = 0$ gap (maximum in *d* wave).

T^* model	*s* wave	*d* wave
$\Delta(n)/\Delta(0)$	$1 - 2n$	$1 - \frac{32}{\pi^3}(3n)^{3/2}$
T^* vs n	$n = 0.94\sqrt{T^*/T_c}\, e^{-1.76 T_c/T^*}$	$T^*/T_c = 2.36 n^{1/2}$

$$\ln\left(\frac{\Delta(n)}{\Delta(0)}\right) = -\frac{8}{\pi}\int_0^{\infty} dy\, y^2 e^{-\Delta(n)y/k_B T^*} \int_0^{\infty} \frac{dx\, e^{-x/k_B T^*}}{\sqrt{x[x + 2\Delta(n)y]}} \tag{22}$$

from which we get

$$\frac{\delta\Delta(n)}{\Delta(0)} = -4\left(\frac{T^*}{\Delta(0)}\right)^3. \tag{23}$$

Also from the definition of n we get immediately

$$n = \frac{\pi^2}{12}\left(\frac{T^*}{\Delta(0)}\right)^2. \tag{24}$$

Exact numerical results agree well with these approximate $n \to 0$ expressions which we summarize in Table II.

In Fig. 6 we show numerical results for $\Delta(n,T)/\Delta(0,0)$

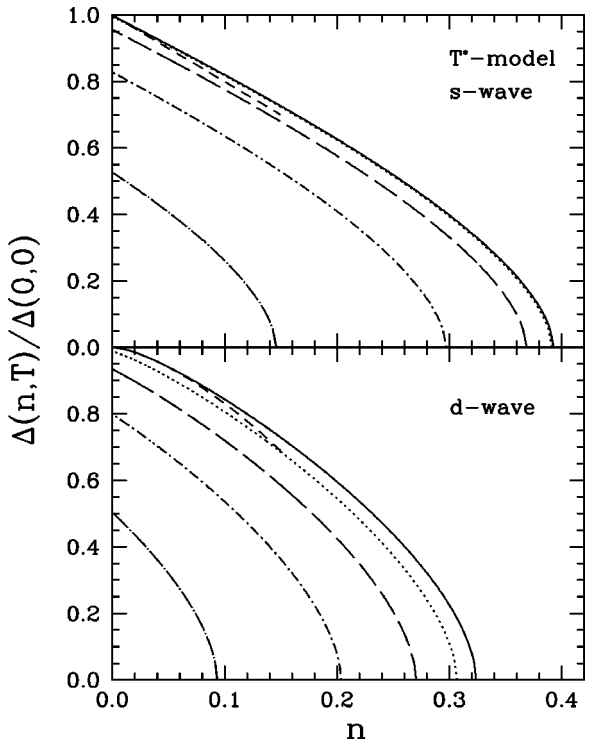

FIG. 6. The ratio of $\Delta(n,T)/\Delta(0,0)$ versus n for finite temperature in the T^* model. The top frame is for an *s*-wave gap and the bottom frame is for *d* wave. Curves are shown for $T/T_c = t = 0.01$ (solid curve), 0.3 (dotted), 0.5 (long-dashed), 0.7 (dot-short-dashed), 0.9 (dot-long-dashed). The short-dashed curve is approximate analytic form for low n given in Table II.

versus n where we have normalized the maximum gap $\Delta(n,T)$ to the zero temperature equilibrium case. The top frame is for s wave while the bottom is d wave. In each frame the short dashed curve is the approximate result at $T=0$ derived above. We see that it compares well with the exact result (solid curve). The other curves apply to $T/T_c=t=0.3$ (dotted), 0.5 (short dashed), 0.7 (long dashed), and 0.9 (dot dashed). In this case the $\Delta(n,T)/\Delta(0,0)$ curves do not cross and are all constructed from BCS curves for the temperature dependence of the gap. The temperature T refers to the sample temperature before the injection of excess quasiparticles n. The intersection of the various curves with the vertical axis simply gives the temperature variation of the gap in BCS. At finite n, the extra quasiparticles are accommodated into the system by assuming a higher temperature thermal distribution T^*, with T^* made sufficiently larger than T to have n extra thermal quasiparticles.

Note that in contrast to the μ^* model, the differences between s and d wave are much less pronounced at $T=0$. This reflects the fact that in a thermal distribution, blocking effects are not an important consideration. In fact now the gap in the d wave case terminates at a value of n which is smaller than in the s wave case. This is opposite to what is found for the μ^* model. Also the curves show no first order transition to the normal state which now occurs only when the gap is zero.

In Fig. 7 we show the value of T^* as a function of the nonequilibrium distribution n for various values of T. The temperatures used are $T/T_c=0.01$, 0.3, 0.5, 0.7, 0.9. Note that the curve with the lowest sample temperature (solid curve) at small n agrees well with our analytic expressions for the same quantity shown as the dashed lines. These follow from the transcendental equation $n=0.94\sqrt{T^*/T_c}e^{-1.76T_c/T^*}$ for s wave and the explicit equation $T^*/T_c=2.36n^{1/2}$ for d wave. These results are also entered in the final line of Table II.

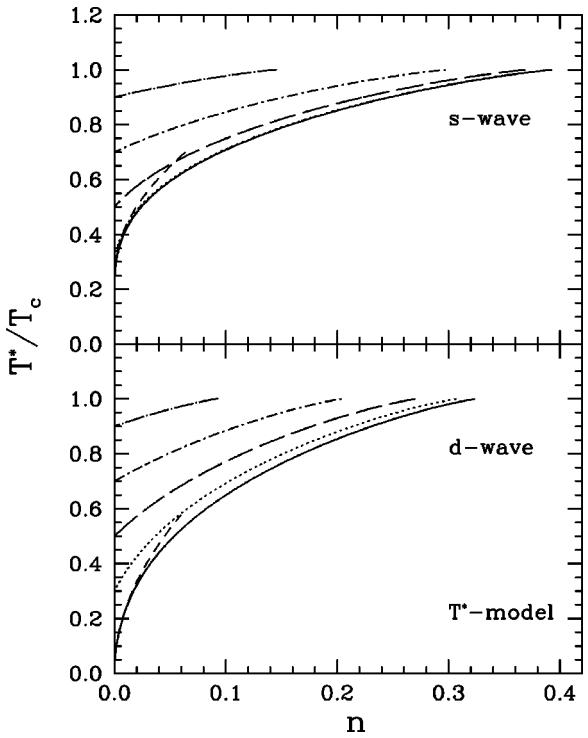

FIG. 7. The parameter T^*/T_c versus n for several temperatures shown for the s-wave (top frame) and d-wave (bottom frame) gaps. Curves are shown for $T/T_c=t=0.01$ (solid curve), 0.3 (dotted), 0.5 (long-dashed), 0.7 (dot-short-dashed), 0.9 (dot-long-dashed). The short-dashed curve is the small n limit (see Table II). T^*/T_c goes to T/T_c as $n\to 0$, which forms the lower limit on the curves with the upper limit being $T^*/T_c=1$ at which point, $\Delta(T^*)$ would be zero.

III. *S-I-N* TUNNELING JUNCTION

Now we consider a specific application of our results to the case of a superconducting-insulator-normal metal tunneling junction. Denote the current in a S-I-N junction with nonequilibrium distribution on the superconducting side, described by the μ^* model, by $I^{SN}_{\mu^*}(V)$ where V is the voltage across the junction. It is given by a straightforward modification of the usual tunneling formula[20]

$$I^{SN}_{\mu^*}(V)=\int_{-\infty}^{\infty}d\epsilon\overline{N}_S(\epsilon)[f(\epsilon-\mu^*)-f(\epsilon+V)], \quad (25)$$

where $\overline{N}_S(\epsilon)$ is the normalized density of states given by

$$\overline{N}_S(\epsilon)=\mathrm{Re}\left\langle\frac{|\epsilon|}{\sqrt{\epsilon^2-\Delta_k^2}}\right\rangle \quad (26)$$

with $\langle\cdots\rangle$ the average over angles as before.

We have seen in the previous section that the introduction of a nonequilibrium μ^* modifies the gap but does not change its symmetry and Eq. (26) still holds for the density of states in Eq. (25) although the new gap amplitude is reduced by a factor of $(1-2n)$ and $(1-4\sqrt{2}n^{3/2}/3)$ for s and d wave, respectively, at zero temperature and n small. In addition to the change in $\overline{N}(\epsilon)$ just described, one of the thermal factors in Eq. (25) is also displaced by the new chemical potential μ^*. The structure of Eq. (25) makes it useful to separate these two factors, and it is convenient to rewrite $I^{SN}_{\mu^*}(V)$ in the form

$$I^{SN}_{\mu^*}(V)=\int_{-\infty}^{\infty}d\epsilon\overline{N}_S(\epsilon)[f(\epsilon-\mu^*)-f(\epsilon)]+\int_{-\infty}^{\infty}d\epsilon\overline{N}_S(\epsilon)[f(\epsilon)-f(\epsilon+V)]. \quad (27)$$

The second term in Eq. (27) has the identical form that applies to an ordinary S-I-N junction in equilibrium at temperature T. We denote the current in this case by $\mathcal{I}(V)$

$$\mathcal{I}(V)\equiv\int_{-\infty}^{\infty}d\epsilon\overline{N}_S(\epsilon)[f(\epsilon)-f(\epsilon+V)], \quad (28)$$

where the gap amplitude defining $\overline{N}_S(\epsilon)$ is that appropriate to the nonequilibrium superconductor. The first term in Eq. (27) is simply a number, independent of voltage. Reference to the defining Eq. (3) for n shows that this number is equal to $n\Delta(0)$. Thus we find

$$I^{SN}_{\mu^*}(V) = \mathcal{I}(V) + n\Delta(0). \tag{29}$$

We see from Eq. (29) that the current voltage characteristics are modified in two ways by the nonequilibrium distribution. The entire equivalent equilibrium distribution is shifted up by an amount $n\Delta(0)$. This allows one to measure n once the gap is known. Secondly, the ''equivalent equilibrium'' current voltage characteristics are those of an equilibrium junction with the smaller nonequilibrium gap used instead of its equilibrium value. This knowledge allows one to fully characterize the nonequilibrium current voltage characteristic and to apply checks to see how well the μ^* model works. For example, the derivative of $I^{SN}_{\mu^*}(V)$ with V at zero temperature simply gives

$$\frac{dI^{SN}_{\mu^*}}{dV} = \overline{N^S}(V), \tag{30}$$

the quasiparticle density of states with the nonequilibrium gap but otherwise it is the same as for an equilibrium distribution. For *s* wave it will have an inverse square root singularity at $\Delta(n)$ and for *d* wave it will go as $\ln[8\Delta(n)/|\Delta(n) - \omega|]/\pi$ instead (see Abanov and Chubukov[21]). In both cases, $\Delta(n)$ can be determined from these singularities. Comparison with its equilibrium value gives a measure of n in both *s* and *d* wave. Next it should be possible to check if this is consistent with the value of the chemical potential related to n by $\mu^*/\Delta(0) = 1 - 2n$ and $\mu^*/\Delta(0) = \sqrt{2}n^{1/2}$, respectively, for *s* and *d* wave, at $T=0$ and in the limit of small n. The chemical potential is measured directly by noting that in Eq. (27) for $V = -\mu^*$, first and second terms on the right-hand side are equal but of opposite sign, giving a sum of zero. In Fig. 8, we show numerical results for $I^{SN}_{\mu^*}(V)$ versus V at a low temperature $T/T_c = 0.1$. The top frame applies to *s* wave while the bottom frame is for *d* wave. It is verified that these curves obey the expected rules mentioned above. For the *s*-wave case $\Delta(n)/\Delta(0)$ is set equal to 0.8 while for the *d*-wave case we have used $\Delta(n)/\Delta(0) = 0.9$ instead. Reference to Fig. 1 for *s* wave and to Fig. 3 for *d* wave shows that these choices correspond to an excess quasiparticle number of approximately 0.09 and 0.12, respectively. The excess quasiparticle number is greater in the *d*-wave case than in *s* wave even though the gap is only reduced by 10% as compared with 20% for *s* wave.

IV. PUMP/PROBE OPTICAL MEASUREMENTS OF $n(T)$

In the following, we wish to discuss recent experimental pump/probe laser experiments which have been used to infer information about the excess quasiparticle density. In particular, we wish to address a claim that these experiments provide evidence for *s*-wave pairing in the high-T_c cuprates. To address this issue, following Kabanov *et al.*,[7] we use the T^* model. While we do not report explicitly on this here, we have also examined these properties within the μ^* model and have found similar results.

To calculate the excess quasiparticle density $n(T)$, we have used Eq. (3) modified for the T^* model via Eq. (4) such that

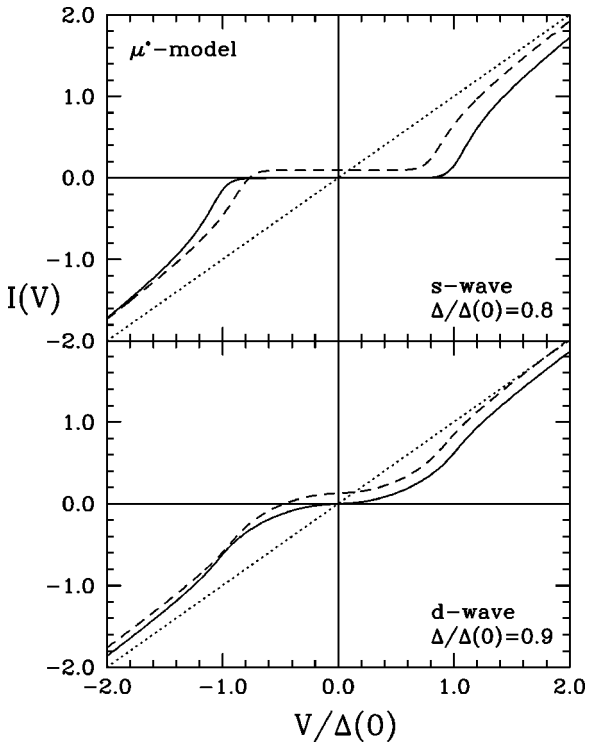

FIG. 8. *S-I-N* tunneling *I-V* characteristics for $T=0$ shown for the μ^* model with *s*-wave gap symmetry (upper frame) and *d*-wave (lower frame). The current I is normalized by $N(0)$ and by the maximum zero-temperature gap in the standard way and the voltage V is normalized to the maximum gap at $T=0$. An excess quasiparticle density n leads to a reduction in the gap by $\Delta(n)/\Delta(0)$ and a vertical shift by n in the *I-V* characteristic. $I=0$ at $V=-\mu^*$. The dotted curve is the normal state $n=0$, the solid curve is superconducting state with $n=0$ and the dashed curve is for a reduced gap $\Delta(n)/\Delta(0)=0.8$ in the *s*-wave case and 0.9 in the *d*-wave case.

$$n(T) = \frac{1}{\Delta(0)}\left\langle \int_0^\infty [f(E_k^*, T^*) - f(E_k, T)]d\epsilon_k \right\rangle, \tag{31}$$

where $E_k^* = \sqrt{\epsilon_k^2 + \Delta_k^2(T^*)}$ (the asterisk always referring to quantities depending on T^* instead of T) and an average over the angle ϕ is done in the case of *d* wave.

To evaluate $n(T)$ at a temperature T, it is necessary to know T^* and $\Delta(T^*)$ and this is determined from the amount of laser energy E_I deposited in the system. In this work, the laser energy will be assumed to go into both electron and phonon systems

$$E_I = \Delta E_{\text{electron}} + \Delta E_{\text{phonon}}. \tag{32}$$

To begin with, however, we examine the case where the energy is assumed to go only into the electronic system: the quasiparticles and a modification of the superconducting condensate due to a $\Delta(T^*)$. The energy going into the quasiparticles relative to the reference nonequilibrium state at temperature T is

$$\Delta E_{\text{qp}} = 4N(0)\left\langle \int_0^\infty [E_k^* f(E_k^*, T^*) - E_k f(E_k, T)]d\epsilon_k \right\rangle. \tag{33}$$

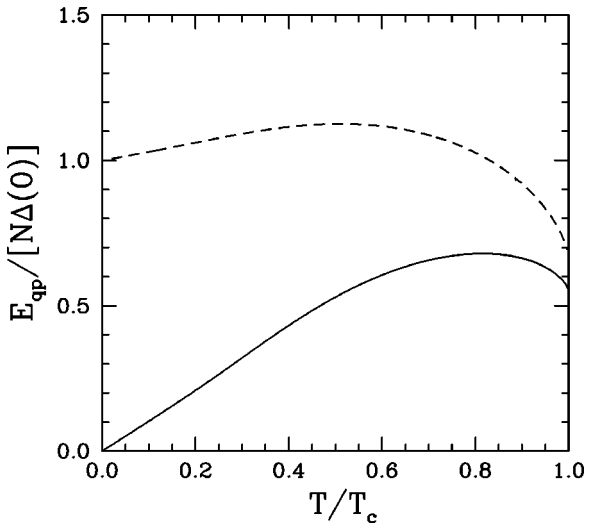

FIG. 9. The average quasiparticle energy per particle normalized to the maximum zero temperature equilibrium gap, $E_{\rm qp}/N\Delta(0)$, versus T/T_c for *s* wave (dashed curve) and *d* wave (solid curve). The $T=0$ value is set by the lowest available energy state in the quasiparticle density of states, whereas near T_c, the energy scale is set by k_BT.

Kabanov *et al.*[7] treated this piece as $[n(T^*)-n(T)](\Delta(T)+k_BT/2)$ which is not completely correct near T_c.

We find that the average quasiparticle energy per particle calculated as

$$\frac{E_{\rm qp}}{N}=\frac{\int_0^\infty E_k f(E_k,T)d\epsilon_k}{\int_0^\infty f(E_k,T)d\epsilon_k} \tag{34}$$

gives a constant equal to $\Delta(0)$ at zero temperature for *s* wave, since excitations can only exist at the gap edge because the density of states is zero below this energy. This behavior is seen in Fig. 9 for the dashed curve which gives Eq. (34) normalized to $\Delta(0)$. As T increases, the energy per particle increases slightly and then decreases near T_c to a value of $\pi^2k_BT_c/12\ln(2)\Delta(0)=1.19[k_BT_c/\Delta(0)]\simeq 0.67$ as now the gap in the quasiparticle density of states has shrunk to zero and the energy of the quasiparticles is controlled by k_BT which is less than $\Delta(0)$. Similar physics is found for a *d*-wave order parameter with the essential difference that excitations can now occur at zero energy and therefore the average quasiparticle energy per particle starts from zero at $T=0$ and rises linearly reflecting the linear increase in energy of the density of states. It can be shown analytically that $E_{\rm qp}/N\Delta(0)\simeq 1.03T/T_c$ for $T\ll\Delta(0)$, the regime where a nodal approximation is valid. At T_c, the quasiparticle energy per particle is once again controlled by k_BT and so the limiting number is given by the same formula as above but with the BCS *d*-wave gap ratio of $\Delta(0)/k_BT_c=2.14$ instead of 1.76 for *s* wave. The number at T_c is approximately 0.55 These results are shown in Fig. 9 (solid curve) and we will refer back to them at a later point.

The reaction of the condensate is simply given as

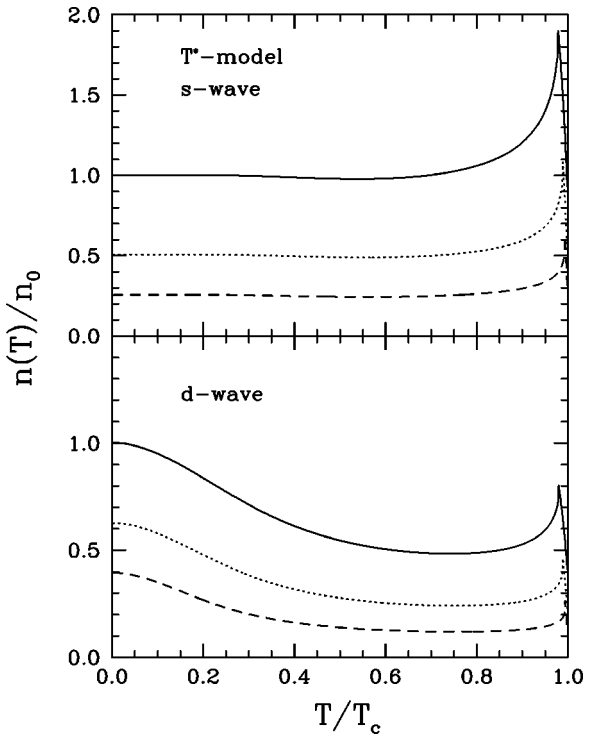

FIG. 10. The excess quasiparticle fraction, $n(T)/n_0$ as a function of T/T_c. These curves are calculated in the T^* model for fixed laser energy, where the energy is assumed to go only into the quasiparticles. The upper frame is for a BCS *s*-wave gap and the bottom frame is for *d* wave. Curves are shown for fixed laser energy E_I (in units of the condensation energy) of 0.2 (solid), 0.1 (dotted), and 0.05 (dashed). Here n_0 is $n(T=0)$ for the case of $E_I=0.2$.

$$\Delta E_{\rm cond}=2N(0)\left\langle\int_0^\infty\left[E_k-E_k^*+\frac{\Delta_k^{*2}}{2E_k^*}[1-2f(E_k^*,T^*)]-\frac{\Delta_k^2}{2E_k}[1-2f(E_k,T)]\right]d\epsilon_k\right\rangle. \tag{35}$$

This term reflects the fact that the presence of excess quasiparticles causes a readjustment to the superconducting condensate through a change in the gap $\Delta^*\equiv\Delta(T^*)$. This term was not included by Parker[13] and neither was it included in the work of Kabanov *et al.*[7]

Our procedure was to fix the laser energy E_I and determine the T^* and $\Delta(T^*)$ which gave $E_I=\Delta E_{\rm qp}+\Delta E_{\rm cond}$. For our purposes, we used the BCS temperature dependence of the gap, calculated numerically, for both $\Delta(T^*)$ versus T^* and $\Delta(T)$ versus T with no approximate form. Our results for both *s*-wave and *d*-wave gap symmetry are shown in Fig. 10 for a variety of E_I, which is normalized to the zero temperature condensation energy in the equilibrium state. Note that the curves shown here are normalized to $n_0\equiv n(T=0)$ for the $E_I=0.2$ case, rather than the $n(0)$ associated with each E_I, in order to show the overall relative reduction as E_I is reduced. For *s* wave, the curves are relatively flat albeit with some small depression followed by a sharp upturn near T_c and then by a drop. The peak occurs when $T^*/T_c=1$, at

which point we assume that the nonequilibrium state has been forced to become a normal metal at an effective temperature T^* and it is measured relative to the equilibrium superconducting state which would exist at temperature T. Therefore, $\Delta E_{\text{electron}}=\Delta E_{\text{electron}}[\Delta^*=0,T^*,\Delta(T),T]$ with T^* being fixed by E_I. Likewise, $n(T)=n[\Delta^*=0,T^*,\Delta(T),T]$. The behavior of the *s*-wave curve largely mimics the inverse of the curve for the energy per quasiparticle. At low temperature, the number of excess quasiparticles is relatively constant with a slight decrease as the temperature is raised, reflecting the fact that the energy per quasiparticle is increasing slightly and so fewer quasiparticles can be created at fixed energy. At high temperature near T_c, the energy per quasiparticle is decreasing and so more quasiparticles can be created for fixed energy and one finds that $n(T)/n(0)$ shows an upturn in response to this. Likewise, the *d*-wave curve for $n(T)/n(0)$ can be understood from the behavior of the E_{qp}/N curve, with the $n(T)/n(0)$ decaying dramatically as T increases reflecting that it is costing on average more energy to create a quasiparticle. We can easily show for the *d*-wave case that

$$\frac{n(T)}{n(0)}=\left(1+\frac{2.9t^3}{E_I}\right)^{2/3}-\left(\frac{2.9t^3}{E_I}\right)^{2/3} \tag{36}$$

for small reduced temperature $t=T/T_c$ with $T\ll\Delta(0)$. For $t\ll E_I$, $n(T)/n(0)\simeq 1-(2.9/E_I)^{2/3}t^2$. For $t\gg E_I$ but still with $T\ll\Delta(0)$, $n(T)/n(0)\simeq(2/3t)(E_I/2.9)^{1/3}$ (inverse t law). Our numerical results conform to these limits. Also note that $n(0)=0.18(E_I/2.9)^{2/3}$ so that $n(T)$ unnormalized to $n(0)$ will go as E_I in the region where the $1/t$ law applies. Once again as the energy scale reverts to k_BT near T_c the slight upturn in $n(T)/n(0)$ is reflecting the smaller energy required to create the quasiparticles. Kabanov *et al.*[7] do not find this result due to their approximations and the details of their curve would differ as they have only included an approximate linear form of the *d*-wave quasiparticle density of states rather than the full form with temperature dependence as is done here. In fact, if their data did not go so low in temperature and given that $n(0)$ is not known experimentally, the flatness of the *d*-wave curve with a slight upturn near T_c placed on an arbitrary scale, would probably make as viable a comparison with their data as the *s*-wave case. However, we note that they do show data at lower temperature and so this interpretation does not hold, also the 2/3 dependence on E_I at $T=0$ is not verified. On the face of things, it may appear that their data agree best with *s*-wave. However, we argue, as they did, that it is necessary to include phonons in this picture.

In their analysis, to obtain agreement with their data, Kabanov *et al.*[7] did include the fact that some of the laser energy would be distributed to phonons in the system. In this case, we partition the laser energy with the phonons as well:

$$E_I=\Delta E_{\text{qp}}+\Delta E_{\text{cond}}+\Delta E_{\text{phonon}}. \tag{37}$$

The phonon piece is calculated assuming that only phonons with energy $\hbar\omega$ above 2Δ can be considered to be out of thermal equilibrium with the lattice and therefore at a temperature T^*. It is in this way that a bottleneck at 2Δ is introduced into the model, which then deviates from pure heating. Such was the same consideration of Kabanov *et al.*[7] As such we calculate the amount of energy going into the phonon system as

$$\Delta E_{\text{phonon}}=\int_{2\Delta}^{\infty}\omega F(\omega)[n(\omega,T^*)-n(w,T)]d\omega, \tag{38}$$

where the usual Bose-Einstein factor $n(\omega,T)=1/[\exp(\hbar\omega/k_BT)-1]$ and $F(\omega)$ is the phonon frequency distribution function measured by Renker *et al.*[22] from neutron scattering experiments on YBCO. In our calculation, we effectively fix $N(0)$ to get the correct ratio of phononic specific heat at T_c relative to the electronic part via comparison with the specific heat data of Loram *et al.*[23] This is to ensure that, the phononic and electronic portions are balanced in accordance with experiment. As the phonon energy increases typically as T^4, one sees that this term, as long as $T^*>T$, will take more and more of the fixed laser energy away from the electronic system and hence, there are fewer excess quasiparticles that can be created at higher temperature and the curve for $n(T)/n(0)$ must go down. This is illustrated in Fig. 11, where curves decay rapidly as T increases and are further reduced for lower E_I. Also shown on the same figure are the experimental results of Kabanov *et al.*[7] (solid squares). We conclude that their data does not support an interpretation of *s*-wave gap symmetry in the high-T_c cuprates. Nor does it agree with *d*-wave (Fig. 10, bottom frame).

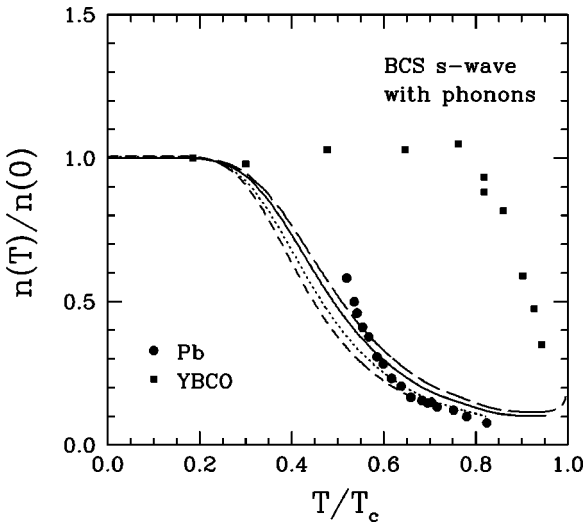

FIG. 11. The excess quasiparticle fraction $n(T)/n(0)$ using a T^* model in *s*-wave including phonons for parameters appropriate to YBCO. For Pb parameters the curves are very similar (and not shown). The curves are for fixed laser energy (in units of the condensation energy) of 0.3 (long-dashed), 0.2 (solid), 0.1 (dotted), and 0.05 (short-dashed). The Pb data of Carr *et al.*, (Ref. 11) reproduced here as the black dots, shows a suppression with increasing T in keeping with our *s*-wave results with phonons. The YBCO data of Kabanov *et al.* (Ref. 7) are shown as the solid squares and disagree with the theory.

We have also done this calculation with the Pb phonon spectrum[24] (adjusted to the specific heat in Pb and using a BCS gap ratio) and we find similar curves to those shown here. The excess quasiparticle density in Pb has been measured by Carr *et al.*[11] and compared successfully to rate equation calculations[25] used for determining the nonequilibrium distribution. We show the Pb data (solid circles) on our curves to emphasize that Pb, as an *s*-wave superconductor, does follow the trend of showing a suppressed excess quasiparticle density as the temperature increases and agrees well with our calculations. This comparison also serves to show that our simple procedure of introducing the bottleneck at 2Δ and sharing the laser energy between phonons and electrons agrees qualitatively and even semiquantitatively with the more sophisticated and accurate rate equation calculations used by Carr *et al.*[11] and validates our simpler method.

Here, we have done the calculation using a BCS gap ratio of 3.53. A full strong coupling Eliashberg calculation[26] would have to be done to include a larger ratio, as from our experience, simply inserting a larger ratio in a BCS calculation can give incorrect, and therefore misleading, results. Aside from the inherent complexity of such a calculation, we would need to commit to some specific mechanism since phonons are not believed to be the source of the high T_c. But there is no consensus on mechanism. To fit experiment, however, Kabanov *et al.*[7] phenomenologically increase the value of the ratio $2\Delta(0)/k_BT_c$ to about 9. There is, however, no rigorous justification for such a procedure and this is our main objection to such a fit. To increase the gap ratio, it is necessary to increase the ratio of $T_c/\omega_{\ln}$ in Eliashberg theory,[26] where $\omega_{\ln}$ is a particular moment of the electron-phonon spectral function which gives the appropriate measure of the average phonon energy involved. When this is done, damping effects, entirely left out of BCS, become dominant and superconducting properties acquire behaviors that are qualitatively different from straightforward extrapolations of BCS behavior (see, for instance, many properties calculated in Ref. 26 in the limit of large $T_c/\omega_{\ln}$ ratio). For YBCO, the gap ratio is closer to 5 (Ref. 27) and is certainly not 9. Further, for a gap ratio ratio of 9–10, the cutoff of 2Δ applied to the phonons falls at 70–80 meV which is at the very top of the measured phonon spectrum.[22] This large value of the cutoff has the effect of greatly reducing the ability of the phonons to share in the laser energy and this partially accounts for why their curve for $n(T)$ in this case stays flat to much higher temperature than for the BCS curve.

V. CONCLUSIONS

In summary, we have examined the differences between an *s*-wave order parameter versus a *d*-wave in a nonequilibrium superconductor using two prominent models in the literature, the T^* model of Parker[13] and the μ^* model of Owen and Scalapino.[14] While these models may be considered to be somewhat crude, they have the virtue of being simple, and accessible in terms of both calculation and physical intuition. As a result, one finds them still being used by experimental groups to aid in the interpretation of their data. With the advent of high-T_c cuprates and the deeper examination of the issue of order parameter symmetry, a re-examination of these models allows for the prediction of different power law dependences on excess quasiparticle density expected between *s*- and *d*-wave gaps. Tables I and II summarize such predictions. These predictions are grounded in interesting physics such as the blocking of states and how the condensate readjusts and as such, they should remain relevant even within more complicated models. It is hoped that the simplicity of our results may inspire further experimental and theoretical efforts to examine nonequilibrium phenomena in the presence of an order parameter with nodes.

In addition, we remind the reader of the past discussions of an inhomogeneous state in the μ^* model and provide the prediction that the *d*-wave state will not be unstable to such a state for the most part. In fact, the *d*-wave state may form a more stable and intuitively interesting state in which to probe nonequilibrium superconductivity.

In our work we have specifically addressed two experiments. *S-I-N* tunneling has always been a powerful probe of *s*-wave superconductors and with our work within the μ^* model, we show how one may use this experiment to measure the model parameters of μ^*, n and $\Delta(n)$ in order to test the predictions of the theory, both for *s*- and *d*-wave cases. The modern use of STM may provide a more attractive avenue for investigating this issue in the face of inhomogeneity where the local density of states may vary with position within the same material.

Finally, recent pump/probe experiments in YBCO which have been interpreted as providing support for *s*-wave gap symmetry[7] are reconsidered. Within a BCS description of the superconducting state and a T^* model for the nonequilibrium distribution, our calculations, including phonons, do not produce an excess quasiparticle distribution $n(T)$ which is nearly constant in temperature with a peak near T_c. Rather a quick decay with increasing T is found as more of the laser energy is taken up by the phonon system. When the explicit case of Pb is considered rather than YBCO, the same rapidly decaying characteristic is found and this is in good agreement with the recent data of Carr *et al.*[11] in this classic *s*-wave superconductor. Our final conclusion is that present pump/probe experiments in YBCO cannot be accounted for by either *s*- or *d*-wave gap symmetry and it may be necessary to reexamine the interpretation of the data in terms of the excess quasiparticle density. In this regard, a next step might be to calculate the optical conductivity itself in the nonequilibrium state so as to make a more direct contact with what is measured.

ACKNOWLEDGMENTS

E.J.N. acknowledges funding from NSERC, Research Corporation, the Government of Ontario (Premier's Research Excellence Award), and the University of Guelph. J.P.C. acknowledges support from NSERC and the CIAR. We thank Larry Carr, David Tanner, David Smith, Ilya Vekhter, and Bernie Nickel for helpful discussions.

[1] *Nonequilibrium Superconductivity*, edited by D.N. Langenberg and A.I. Larkin (North-Holland, New York, 1986).
[2] N. Kopnin *Theory of Nonequilibrium Superconductivity* (Clarendon Press, Oxford, 2001).
[3] A.M. Gulian and G.F. Zharkov *Nonequilibrium Electrons and Phonons in Superconductors* (Plenum, New York, 1999).
[4] P.B. Allen, Phys. Rev. Lett. **59**, 1460 (1987).
[5] S.D. Brorson, A. Kazeroonian, J.S. Moodera, D.W. Face, T.K. Cheng, E.P. Ippen, M.S. Dresselhaus, and G. Dresselhaus, Phys. Rev. Lett. **64**, 2172 (1990).
[6] S.G. Han, Z.V. Vardeny, K.S. Wong, O.G. Symko, and G. Koren, Phys. Rev. Lett. **65**, 2708 (1990); G.L. Eesley, J. Heremans, M.S. Meyer, G.L. Doll, and S.H. Liou, *ibid.* **65**, 3445 (1990); J.M. Chwalek, J.F. Whitaker, G.A. Mourou, J. Agostinelli, and M. Lelental, Appl. Phys. Lett. **57**, 1696 (1990); S.D. Brorson, A. Kazeroonian, D.W. Face, T.K. Cheng, G.L. Doll, M.S. Dresselhaus, G. Dresselhaus, E.P. Ippen, T. Venkatesan, X.D. Wu, and A. Inam, Solid State Commun. **74**, 1305 (1990).
[7] V.V. Kabanov, J. Demsar, B. Podobnik, and D. Mihailovic, Phys. Rev. B **59**, 1497 (1999); D. Mihailovic and J. Demsar, in *Spectroscopy of Superconducting Materials*, edited by Eric Faulques, ACS Symposium Series No. 730 (The American Chemical Society, Washington, D.C., 1999), p. 230.
[8] We are not able to refer to all possible references here, but rather give a couple for illustration of some of the interesting features that have been examined, such as coherent phonon oscillations: J.M. Chwalek, C. Uher, J.F. Whitaker, G.A. Mourou, and J.A. Agostinelli, Appl. Phys. Lett. **58**, 980 (1991); W. Albrecht, Th. Kruse, and H. Kurz, Phys. Rev. Lett. **69**, 1451 (1992).
[9] V.V. Kabanov, J. Demsar, and D. Mihailovic, Phys. Rev. B **61**, 1477 (2000); J. Demsar, R. Hudej, J. Karpinski, V.V. Kabanov, and D. Mihailovic, *ibid.* **63**, 054519 (2001).
[10] C.J. Stevens, D.C. Smith, C. Chen, J.F. Ryan, B. Podobnik, D. Mihailovic, G.A. Wagner, and J.E. Evetts, Phys. Rev. Lett. **78**, 2212 (1997); R.A. Kaindl, M. Woerner, T. Elsaesser, D.C. Smith, J.F. Ryan, G.A. Farnan, M.P. McCurry, and D.G. Walmsley, Science (Washington, DC, U.S.) **287**, 470 (2000).
[11] G.L. Carr, R.P.S.M. Lobo, J. LaVeigne, D.H. Reitze, and D.B. Tanner, Phys. Rev. Lett. **85**, 3001 (2000).
[12] Some recent examples are B.J. Feenstra, J. Schützmann, D. van der Marel, R. Pérez Pinaya, and M. Decroux, Phys. Rev. Lett. **79**, 4890 (1997); R.D. Averitt, G. Rodriguez, A.I. Lobad, J.L.W. Siders, S.A. Trugman, and A.J. Taylor, Phys. Rev. B **63**, 140502(R) (2001).
[13] W.H. Parker, Phys. Rev. B **12**, 3667 (1975).
[14] C.S. Owen and D.J. Scalapino, Phys. Rev. Lett. **28**, 1559 (1972).
[15] W.H. Parker and W.D. Williams, Phys. Rev. Lett. **29**, 924 (1972).
[16] J.J. Chang and D.J. Scalapino, Phys. Rev. B **10**, 4047 (1974).
[17] D.J. Scalapino and B.A. Huberman, Phys. Rev. Lett. **39**, 1365 (1977).
[18] R.C. Dynes, V. Narayanamurti, and J.P. Garno, Phys. Rev. Lett. **39**, 229 (1977); K.E. Gray and H.W. Willemsen, J. Low Temp. Phys. **31**, 911 (1978); I. Iguchi and D.N. Langenberg, Phys. Rev. Lett. **44**, 486 (1980); S. Kotani, Y. Yamaki, and I. Iguchi, Physica B **107**, 535 (1981); Chong-De Wei, Xiao-Lan Luo, and Xiao-Fan Meng, *ibid.* **107**, 537 (1981); H. Akoh and K. Kajimura, *ibid.* **107**, 537 (1981); Phys. Rev. B **25**, 4467 (1981); I. Iguchi and Y. Suzuki, *ibid.* **28**, 4043 (1983).
[19] See, for instance, A.L. Fetter and J.D. Walecka, *Quantum Theory of Many-Particle Systems* (McGraw-Hill, New York, 1971), Eq. (51.46a), p. 449.
[20] For example, see R. Merservey, and B.B. Schwartz, in *Superconductivity*, edited by R.D. Parks (Marcel Dekker, New York, 1969), Vol. 1, p. 134.
[21] Ar. Abanov and A.V. Chubukov, Phys. Rev. B **61**, R9241 (2000).
[22] B. Renker, F. Gompf, E. Gering, N. Nücker, D. Ewert, W. Reichart, and H. Rietschel, Z. Phys. B: Condens. Matter **67**, 15 (1987).
[23] J.W. Loram, K.A. Mirza, J.R. Cooper, W.Y. Liang, and J.M. Wade, J. Supercond. **7**, 243 (1994).
[24] For convenience, we have used the Pb $\alpha^2F(\omega)$ spectrum scaled to give the correct specific heat, rather than the $F(\omega)$ as the two are very similar. The Pb $\alpha^2F(\omega)$ is given by W.L. McMillan and J.M. Rowell, in *Superconductivity*, edited by R.D. Parks (Marcel Dekker, New York, 1969), Vol. 1, p. 601. A comparison between the tunneling $\alpha^2F(\omega)$ spectrum and $F(\omega)$, as derived from neutron scattering, is reproduced in Ref. 26, p. 1058.
[25] S.B. Kaplan, C.C. Chi, D.N. Langenberg, J.J. Chang, S. Jafarey, and D.J. Scalapino, Phys. Rev. B **14**, 4854 (1976).
[26] For example, J.P. Carbotte, Rev. Mod. Phys. **62**, 1027 (1990).
[27] For example, T. Hasegawa, H. Ikuta, and K. Kitazawa, in *Physical Properties of High T_c Superconductors III*, edited by D.M. Ginsberg (World Scientific, Singapore, 1992), p. 525; E. Schachinger, J.P. Carbotte, and D. Basov, Europhys. Lett. **54**, 380 (2001): J.W. Loram, K.A. Mirza, J.P. Cooper, W.L. Liang, and J.M. Wade, J. Supercond. **7**, 243 (1994); M. Gurvitch, J.M. Valles, Jr., A.M. Cucolo, R.C. Dynes, J.P. Garno, L.F. Schneemeyer, and J.V. Waszczak, Phys. Rev. Lett. **63**, 1008 (1989); A.G. Sun, L.M. Paulius, D.A. Gajewski, M.B. Maple, and R.C. Dynes, Phys. Rev. B **50**, 3266 (1994); M. Aprili, E. Badica, and L.H. Greene, Phys. Rev. Lett. **83**, 4630 (1999); M. Aprili, M. Covongton, E. Paraoanu, B. Niedermeier, and L.H. Greene, Phys. Rev. B **57**, R8139 (1998); J.Y.T. Wei, N.-C. Yeh, D.F. Garrigus, and M. Strasik, Phys. Rev. Lett. **81**, 2542 (1998); Y. Dagan, R. Krupke, and G. Deutscher, Phys. Rev. B **62**, 146 (2000).